Numerical Simulation of the Reactive Two-Phase Solid Rocket Motor Exhaust Plume

Zheng Li
School of Astronautics
Beijing University of Aeronautics and Astronautics
Beijing, China
roy_lizheng@hotmail.com

Hongjun Xiang
School of Astronautics
Beijing University of Aeronautics and Astronautics
Beijing, China
hjxiang@263.net

***Abstract*—This study is focused on numerical simulation of the reactive two-phase flow from the end of the motor combustion chamber to the exhaust plume. The NASA computer program CEA (Chemical Equilibrium with Applications) has been used to calculate the equilibrium composition of AP/HTPB/Al composite propellant in the chamber. Then the 2D Navier-Stokes equations with additional terms describing turbulence, chemical kinetics and gas-particle (Al_2O_3) interaction have been solved for numerical simulation of plumes at an altitude of 10 km. AUSM (Advection Upstream Splitting Method) vector splitting method and a second order upwind-biased scheme are present in the calculation. The resulting diagrams of temperature and mass fraction of components in the plume and profiles on the axis are shown. The flow field structure and particle behavior in the plume is discussed. Especially, the ability of coupled computation to represent complex physics phenomena of this kind is demonstrated.**

Keywords-solid rocket motor; numerical simulation; plume; reactive;two-phase flow

I. INTRODUCTION

Rocket exhaust plumes have been a subject of intensive interdisciplinary study during the last decades [1]-[7]. Thermodynamics of the propellant, fluid dynamics of the chemically reacting mixture of gaseous and particulate species and the radiative transport of the nonhomogeneous emitting and scattering flow field is contained in the exhaust plume phenomenology. A description of the major kinetic and optical processes in solid engine exhaust flows is given in [8].

The exhaust plume is formed by rapid expansion through an exhaust nozzle of high pressure combustion products contained in the chamber. The resulting plume is composed of gaseous species and particles in a condensed phase. Some of these partially unburned products can react with oxidizing species contained in the ambient air to form the afterburning phenomenon. This phenomenon changes the structure, temperature and component of the exhaust plume flow field. The computation of infrared signatures is usually done by the use of a radiative code chained with a flow field (CFD) code. Thus, the accuracy of the flow field is predominant for the final radiative result: the physics of the simulation needs to be realistic and input parameters must be well defined.

The aim of this paper is to characterize the flow field of the exhaust plume with fixed assumptions, putting the emphasis on the use of existant modelization tools. Two comparisons are made to describe the influence of the reaction and particles phase. The ability of coupled computation to represent complex physics phenomena of this kind is demonstrated.

II. COMPUTATION DESCRIPTION

A. Domain and grids

The geometry used in the computations consists of a Laval nozzle and the external plume flow field. The computational domain is treated as 2D axisymmetric with a quadrilateral elements grid partition. It is chosen to be 0.2m upstream and 3m downstream to avoid spurious reflections on its far-field boundaries. The nozzle grid has 96×32 cells with a small refinement in the shearing zone. And the plume zone has 90×300 cells. A grid consisting of 30572 cells were used. Fig.1 displays all these grids.

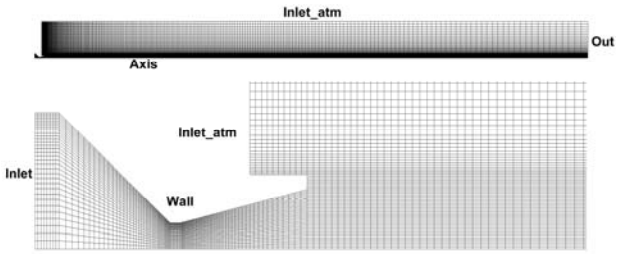

Figure 1. Structure grid of the nozzle and plume field.

B. Models

1) Thermodynamics

The reacting multiphase flow in the solid rocket chamber can be effectively treated as consisting of a continuous phase composed of the products of combustion from the binder (HTPB), the ammonium perchlorate (AP), and reacted aluminum, and a discrete phase composed of particles containing aluminum and Al_2O_3. The physics of metalized propellant combustion includes diffusion transfer controlled combustion of agglomerates as well as gas-phase reactions. The kinetic timescales associated with the reactions in the continuous phase, however, are likely to be small compared to the fluid dynamics timescales in the chamber. The continuous-phase chemistry can, therefore, be treated using chemical equilibrium. The CEA (Chemical

Published by Atlantis Press, Paris, France.

Equilibrium with Applications) program [9] calculates chemical equilibrium product concentrations of the compose propellant which is consists of 68% AP, 20% Al and 12% HTPB. The result of calculation will be the input of the flow field.

2) Flowfield calculation

The numerical solution of the Navier-Stokes equations for a chemically reacting gas flow has been obtained with finite volume spatial discretization on a structured 2D grid implemented in FLUENT. The solution was generated for the conditions of 10 km altitude. ASUM (Advection Upstream Splitting Method) vector splitting method is used for the convective fluxes. The second-order upwind-biased scheme with an additional limiter is applied for the spatial reconstruction of volume properties in the cell boundaries. The realizable k-ε turbulence model is included to model the effects of turbulence. With the initialization of FMG method, the computation has been significant accelerated.

The exhaust gases generated by the combustion of composite propellant consist primarily of HCl, CO, and H_2. Because of the high temperature and the shear layer, chemical reactions occur between exhaust and atmospheric species that affecting the flow field. To represent the reacting flow within the rocket nozzle and exhaust plume, a finite-rate chemical kinetics model is included in the analysis. Seventeen elementary reactions involving twelve chemical species (N=12) are considered in the combustion model. The chemical species used are H_2, O_2, H_2O, H, O, OH, HCl, Cl_2, Cl, CO, CO_2, and N_2 (an inert). The seventeen reaction model [10] used for the finite-rate chemistry is given in table 1.

TABLE I. THE SEVENTEEN REACTION MODEL

Reaction	A(cm3/mol·s)	n	E(j)
$H+O_2=OH+O$	1.915E+14	0	7.03E+04
$O+H_2=H+OH$	5.080E+04	2.67	2.63E+04
$OH+H_2=H+H_2O$	2.160E+08	1.51	3.43E+04
$OH+OH=O+H_2O$	1.506E+09	2.02	1.34E+04
$H+H+M=H_2+M$	4.577E+19	-1.4	1.04E+05
$H+OH+M=H_2O+M$	1.912E+23	-1.83	1.18E+05
$H+O+M=OH+M$	9.880E+17	-0.74	1.02E+05
$O+O+M=O_2+M$	4.515E+17	-0.64	1.19E+05
$CO+OH=CO_2+H$	9.420E+03	2.25	-2.35E+03
$CO+O_2=CO_2+O$	2.499E+12	0	4.77E+04
$CO+O+M=CO_2+M$	6.170E+14	0	3.00E+03
H+HCL=H2+Cl	1.692E+13	0	4.14E+03
H+CL2=HCL+Cl	8.551E+13	0	1.17E+03
HCL+OH=H2O+Cl	2.710E+07	1.65	-2.2E+02
HCL+O=OH+Cl	3.370E+03	2.87	3.51E+03
$Cl+Cl+M=Cl_2+M$	4.675E+14	0	-1.8E3
H+Cl+M=HCl+M	1.192E-02	-2	0

Particles of alumina (aluminum oxide, Al_2O_3) are primarily encountered in the exhausted of solid propellant rocket; finely ground aluminum powder is mixed specific impulse, while also serving to stabilize the combustion. These particles can easily affect the final structure and radiation properties of the plume [8]. A Lagrangian approach is used here for the computation of particle concentrations and temperature fields from the gaseous turbulent gas phase field. The inlet section of the computational domain is subdivided into elementary surfaces and individual particles are injected through these surfaces. The mass fraction of Al_2O_3 listed in Table 2 is 34.055%. Seven groups of particles have been added into the flow field with 5μm average diameter.

Several modeling assumptions are made:

- No phase change is considered for the particles that are considered to be always liquid
- The turbulent dispersion effects are neglected
- No interaction between the 7 groups of particles
- The size, velocity and temperature in each group is uniform

C. Boundary conditons

The nozzle inlet is treated with total pressure, total temperature, and uniform axial injection of considered chemical species computed by CEA. A pressure-far-field condition is used at the freestream inflow. The mass friction at the chamber exit plane and freestream ambient conditions are summarized in tables 2 and 3. The axis is defined as symmetry, while no-slip walls are considered still and adiabatic. Finally, the outlet is subsonic and atmospheric pressure is prescribed.

TABLE II. MASS FRACTIONS OF CHEMICAL SPECIES

Species	Freestream	Nozzle inlet
CO	0.00000	0.23539
CO_2	0.00030	0.014314
CL	0.00000	0.012677
CL_2	0.00000	0.000052696
H	0.00000	0.0012654
HCl	0.00000	0.17732
H_2	0.00000	0.022699
H_2O	0.00000	0.064548
N_2	0.78953	0.127671
O	0.00000	0.0001868
OH	0.00000	0.0032805
O_2	0.21017	0.000045804
$Al_2O_3(L)$	0.00000	0.34055

TABLE III. FLOW CONDITIONS

	Velocity (m/s)	Pressure (Pa)	Temperature (K)
Freestream	650	26500	216.65
Nozzle	/	7000000	3461.35

III. RESULTS

A. Computation of the gas phase

The fuel-rich plume is exposed to the atmosphere, which is not an inert chemical background, but allows additional oxidant to react with exhaust gases. It is important to focus on the chemical reaction of the exhaust plume, because it dominates the temperature and mass friction field which is the key point in the infrared radiation computation. Some comparisons between with and without reaction have been made to represent the influence of the chemical reaction in the exhaust plume.

The global flow structure of gas is illustrated by the temperature field (see Fig. 2). The similar structure has been

obtained in the two cases. The exhaust gas produced at the combustion chamber is accelerated by the Laval nozzle corresponding to a temperature decrease. As the exhaust gas out of the nozzle, expansions and compressions of the plume is shaped by the ambient pressure. Surrounding core flow, the viscosity effects permit the development of the mixing of fast exhaust gases with slower freestream air. As we can see in the reaction case, temperature is a little higher than the inert case at the expansion section of the nozzle. There is a slight difference in the core flow between the two cases. However, a high temperature tape is obtained at the mixing layer in the reaction case. The mixing layer is reheated by the reaction which takes place at the suitable temperature and concentration of the exhaust gas.

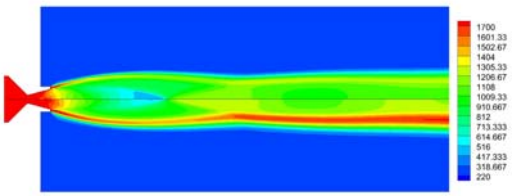

Figure 2. Comparison of flow field temperature (upper: reaction, lower: inert).

Fig. 3 gives a comparison of the temperature with and without reaction. The axial temperature (Fig. 3a) oscillations correspond to the expansion/compression zone with the same shape in two cases. One can see a slight difference between the two cases in the nozzle and near the outlet of the nozzle. But after that a significant difference has been obtained which reaches the maximum in the region near x=1.5 m. It can be explained by the fact that in the flow field, the reaction between exhaust gas and air reheated the plume. As the effect of mixing improving along the axis, the reaction has occurred closer to the axis and has more influence to axial temperature. Fig. 3b compares the temperature between the two cases at x=1m. As we can see in Fig. 3b the maximum temperature is gained in the mixing layer near y=0.02m where the reaction takes place. And the temperature drops to the ambient condition out of y=0.1m. Comparing to the inert case, additional heat increment is also indicated in Fig. 3b.

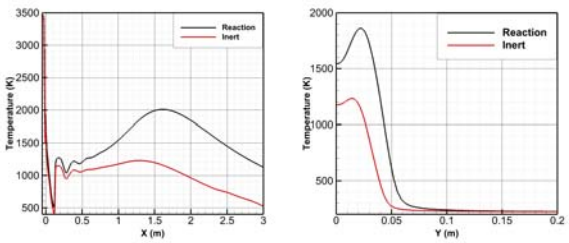

(a) Axis (b) X=1 m

Figure 3. Comparison of temperature.

Fig. 4 compares mass fractions of H_2, HCl, CO and H_2O species along the axis. The first three ones are the main partially unburned species in the chamber that are injected at the nozzle inlet. After oscillations due to the expansion/compression zones, the mass fractions all fall down at about x=0.5 m in the two cases because of the mixing between exhaust plume and air. In the reaction case, the unburned species decreases a little faster than the inert case. In the meantime, the increase of H_2O production is obtained in the reaction case, corresponding to the consumption of H_2.

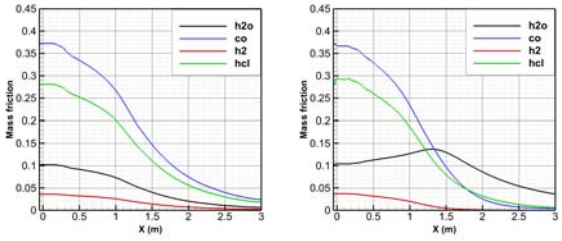

(a) Reaction (b) Without reaction

Figure 4. Mass friction on the axis.

Fig. 5 gives a comparison of the OH mass friction distribution in the afterburning zone. As we can see in the inert case, the OH mass fraction is vanishing along the axis because of the mixing between exhaust plume and air. To the contrary, a strong production of OH is gained in the downstream of the plume in the other case. In the reaction 1 to 8 show at Table 1, OH is known as an intermediate for combustion and thus it determines afterburning flame in the mixing layer. At some distance downstream the production of OH is then burned and transformed to H_2O. Fig. 6 shows the two CO_2 mass friction structures in the plume. In the carbon monoxide combustion, CO_2 is directly produced from CO. Contrary to the inert case, the CO_2 mass friction is up to 0.1 at the downstream of reactive plume. The maximum of OH and CO_2 is determined by the necessity of the air/exhaust mixture to be heated to a temperature at which combustion can occur. Fig. 7 indicates the difference of the Cl mass fraction between the two cases. Differing from the two species shown above, HCl is decomposed to Cl and Cl_2 in the nozzle. Cl is produced nearly instantaneously in the mixing layer next to the exit nozzle.

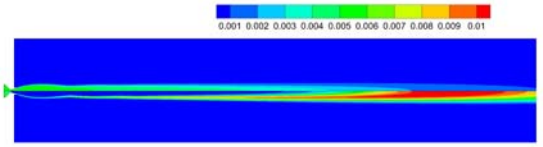

Figure 5. Comparison of OH mass friction in the after burning zone (upper: reaction, lower: inert).

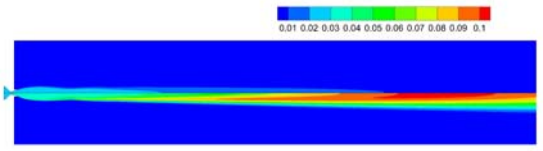

Figure 6. Comparison of CO_2 mass friction in the after burning zone (upper: reaction, lower: inert).

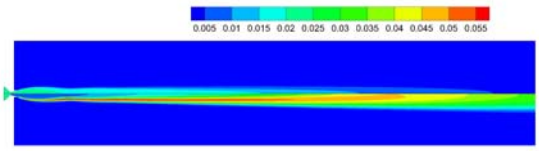

Figure 7. Comparison of Cl mass friction in the after burning zone (upper: reaction, lower: inert).

B. *Two-phase flow simulation*

The numerical simulation on the two-phase flow of the exhaust plume is based on the calculation of the reactive flow. Seven groups of particles (Al_2O_3) are injected at the nozzle inlet with different size. The flow structure is showed in Fig. 8. Comparing with Fig. 2 which is not considering the particle influence, the two-phase flow contains a higher temperature zone up to 3000K in the oscillation area. In the particles case, the core flow of gas-phase is reheated by particle flow. Fig. 9 compares the temperature of axis between the cases with and without particles. One can see that there is a big difference in the expansion/compression zone at x=0 m to x=1.5 m. Contrary to the gas-phase, the particles (Al_2O_3) which are not affected with the compressibility are better in preserving heat.

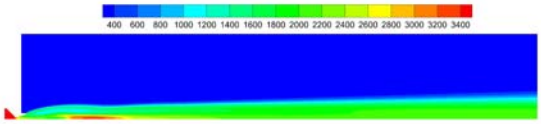

Figure 8. The temperature contours of two-phase flow case.

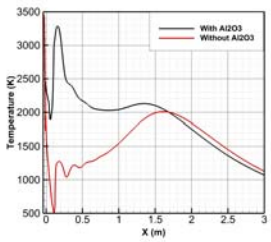

Figure 9. Comparison of axis temperature.

IV. CONCLUSION

A numerical scheme has been developed that can calculate the flow in an intermediate altitude solid rocket exhaust plume with the AP/HTPB/Al composite propellant. The combustion chamber condition as the input of the flow simulation is calculated by the NASA CEA program. And the exhaust plume is described by solving the 2D Navier-Stokes equations in FLUENT. Included in the analysis are nonequilibrium chemical reactions, gas-particle interaction and turbulence in the mixing layer. Two comparisons are made to describe the influence of reaction and particles:

- Reactions occurring at the mixing layer would reheat the plume and change its component. Up to 850K heat increment is obtained in the reaction case. The mass friction of H_2O would increase. And the mass friction of CO, HCl and H_2 decrease a little faster.
- The Al_2O_3 particles generated by the combustion of solid propellant will reheat the core flow of the exhaust plume at the expansion/compression zone.

The final achievement would be to account for some radiative computation permitting the evaluation of the infrared emission of gases such as H_2O, CO_2, CO and HCl and of alumina particles, in order to entirely validate the assumptions made for the aerothermochemical calculations.

REFERENCES

[1] Hong, J. S., Levin, D. A., Collins, R. J., Emery, J., and Tietjen, A., "Comparison of Atlas ground-based plume imagery with chemically reacting flow," AIAA Paper 97-2537, June 1997.

[2] P. J. Coelho, Numerical simulation of the interaction between turbulence and radiation in reactive flows, Progress in Energy and Combustion Science 33 (2007) 311-383

[3] Rao, R. M., Sinha, K., Candler, G. V., Wright, M. J., and Levin, D. A., "Numerical Simulation of Atlas II Rocket Motor Plumes," AIAA Paper 99-2258, June 1999.

[4] Reis, R. J., Aucoin, P. J., and Stechman, R. C., "Prediction of rocket exhaust flowfields," Journal of Spacecraft and Rockets, Vol. 7, No. 2, Feb. 1970, pp. 155-159.

[5] Reed, R. A., and Calia, V. S., "Review of aluminum oxide rocket exhaust particles," AIAA Paper 93-2819, 1993.

[6] Burt, J. M., and Boyd, I. D., "Particle rotation effects in rarefied two phase plume flows," 24th International Symposium on Rarefied Gas Dynamics, Monopoli, Italy, 2004

[7] Candler, G., Rao, R., Sinha, K., and Levin, D., "Numerical simulations of Atlas II rocket plumes," AIAA Paper 2001-0354, Jan. 2001

[8] Simmons, F. S., Rocket exhaust plume phenomenology, Aerospace Press, EI Segundo, CA, 2000.

[9] http://www.grc.nasa.gov/WWW/CEAWeb/

[10] J. Troyes, I. Dubois, V. Borie, A. Boischot, Multi-phase reactive numerical simulations of a model solid rocket motor exhaust jet, AIAA 2006-4414